

to KACG'99 Proceedings

## TSSG-pulling of Sillenite $\text{Bi}_{12}\text{TiO}_{20}$ for EOS Application

Shintaro MIYAZAWA\*

USHIO Research Institute of Technology (URIT) Inc.,

USHIO INC.

1-90, Komakado, Gotenba-shi, Shizuoka 412-0038, Japan

Foot Note-----

\*E-mail address : miyazasn@mail.ushio.co.jp

-----  
**Key Words ;**  $\text{Bi}_{12}\text{TiO}_{20}$ , phase diagram, TSSG-pulling, solid solution, stoichiometry, sillenite,

electro-optic sampling, refractive index

**ABSTRACT**

The reproducibility of successive growth of  $\text{Bi}_{12}\text{TiO}_{20}$  (BTO) single crystals using a top-seeded solution growth (TSSG) pulling method was evaluated by measuring the lattice constants and their standard deviations. A substantial phase diagram in the region close to the stoichiometric BTO was established experimentally for this purpose, and the existence of a retrograde solid solution close to a BTO was clarified. It was emphasize that a starting solution, with a 10.0~10.1 mol%  $\text{TiO}_2$  concentration, results in large single crystals with a highly homogeneous lattice constant of within  $\pm 1 \times 10^{-4} \text{ \AA}$ , when the solidified fraction of the grown crystal is less than about 45%.

A wavelength dispersion of refractive index was measured for the first time, and it was verified that the refractive index of BTO is larger than that of BSO ( $\text{Bi}_{12}\text{SiO}_{20}$ ), allowing the voltage sensitivity of EOS higher than the case with BSO as a probe head.

## 1. Introduction

A high-impedance electro-optic sampling (EOS) prober has already become a standard tool in measuring the ultrafast electrical signals in printed circuits and multi-chip modules now being applied to mobile communications and data transmission<sup>1,2</sup>). More recently, a novel handy-type, high-impedance probing system consisting of an electro-optic  $\text{Bi}_{12}\text{SiO}_{20}$  (BSO) crystal was developed for measuring multi-GHz signals<sup>3</sup>).

However, its voltage sensitivity must be further improved in practices. The shot-noise-limited expression for the minimum detectable voltage  $V_{\min.}$  in the EOS technique<sup>1</sup>) is expressed as

$$V_{\min.} = 4 V_{\pi} / \pi \cdot \sqrt{q / i_{\text{avg}}}, \quad (1)$$

where  $V_{\pi}$  is the half-wave voltage of the electro-optic crystal,  $q$  is electron charge, and  $i_{\text{avg}}$  is the average photocurrent of the system's photodetector. Because  $V_{\pi}$  is inversely proportional to  $n^3r$ , the product of electro-optic constant  $r$  and refractive index  $n$ , the sensitivity can be increased by using an electro-optic crystal with a larger  $r_{41}$  and  $n$  than those of a BSO crystal.

Then, we turned our attention to  $\text{Bi}_{12}\text{TiO}_{20}$  (BTO) single crystals for use in an EOS probe head, because they have the largest electro-optic constants  $r_{41}$  among sillenites so far reported<sup>4</sup>), although the precise value of their refractive index is unknown.

According to the phase diagram of the  $\text{Bi}_2\text{O}_3\text{-TiO}_2$  binary system reported by Bruton<sup>5</sup>), BTO melts incongruently at 873~875°C, decomposing into liquid and  $\text{Bi}_4\text{Ti}_3\text{O}_{12}$  associated with a peritectic reaction and the single phase BTO does not have any solid solution. Therefore, BTO single crystals are usually grown using the top-seeded solution growth (TSSG) pulling method from  $\text{Bi}_2\text{O}_3$ -rich solutions of less than about 12 mol%  $\text{TiO}_2$ , far from the stoichiometric BTO (14.286 mol%  $\text{TiO}_2$  composition)<sup>6,7,8,9,10</sup>). However, a standard method for growing BTO single crystals has not yet been established.

This paper primarily discusses a phase relation in a  $\text{Bi}_2\text{O}_3$ -rich region from the stoichiometric composition and BTO single crystal growth using the TSSG method based on a substantial phase diagram. The phase diagram reported earlier<sup>5)</sup> was renewed experimentally. Moreover, a wavelength dispersion of the refractive index was measured for the first time and a sensitivity improvement in the EOS system, using a BTO crystal, is discussed briefly in comparison with the case of a BSO.

## 2. Experimental

Ultra-high purity raw materials of  $\text{Bi}_2\text{O}_3$  (99.9995%) and  $\text{TiO}_2$  (99.995%) were used throughout this work. In drawing a substantial phase diagram close to the stoichiometric BTO (14.28<sub>6</sub> mol%  $\text{TiO}_2$ ), a differential thermal analysis (DTA) of binary compounds with different  $\text{TiO}_2$  concentrations close to the stoichiometric composition was carried out in order to reexamine the peritectic reaction and eutectic temperatures. Heating and cooling rates were 1°C/min. To clarify the peritectic composition experimentally, TSSG pulling was carried out with solutions that varied between 10.25 and 11.25 mol%  $\text{TiO}_2$ .

To examine the existence of a solid solution range close to the stoichiometric BTO phase, mixed binary compounds with 13.3~14.7 mol%  $\text{TiO}_2$  were calcined at  $830 \pm 5^\circ\text{C}$  for 20 hr in air, and the lattice constants of the BTO phase in each ceramic were evaluated. The calcination temperature of the ceramics was very close to the determined eutectic temperature described hereafter, resulting in sufficient precipitation of the BTO phase. They were analyzed by X-ray powder diffractometry using  $\text{K}\alpha_1$  at room temperature with Si powder as a reference and were calculated by means of the Nelson-Riley approximation method using all peaks indexed to the cubic sillenite BTO. The measurements were carried out more than 3 times for each compound, and measurement accuracy was estimated to be less than  $1 \times 10^{-4} \text{ \AA}$ .

Single crystals of BTO were grown using a TSSG technique from off-stoichiometric solutions with starting compositions of 4.0, 5.0, 6.5, 8.0, 9.0, and 10.25 mol%

$\text{TiO}_2$ . Growth apparatus has already been reported elsewhere<sup>9)</sup>, and only the essential growth conditions are briefly given here:  $\sim 0.25$  mm/hr pulling rate, 35~45 rpm crystal rotation rate, oxygen atmosphere (about 2 l/min flow) during the pulling, and about 350 gr total amount charged in a 40 cc Pt crucible. In this study, the pulling axis was fixed to the [100] direction. Three to five single crystals, typically 15~20 mm in diameter and about 25 mm in length, typically weighing about  $\sim 40$  gr, were grown in succession from one starting solution. For successive growth from the initial solution, calcined stoichiometric BTO ceramics, equal in weight to that of the previously grown crystal, were added to the residual solution. The grown crystals were also characterized by their lattice constants estimated with X-ray powder diffractometry and the Nelson-Riley approximation method in the same manner. Samples were prepared from the first crystallized part immediately below the seed crystal. Further growth experiments of relatively long single crystals were carried out with 9.0 and 10.0 mol%  $\text{TiO}_2$  solutions to examine the change in lattice constants along the crystal. The change is discussed using the substantial phase diagram renewed here.

An accurate refractive index of a BTO has not been reported so far, so the wavelength dispersion of the refractive index was measured by means of the minimum deviation method using a prism.

### 3. Results and discussion

#### 3.1 Phase diagram

Figure 1(a) shows the substantial phase diagram drawn by the experimental results described below. On DTA curves of ceramics with different mol%  $\text{TiO}_2$ , strong exothermic and endothermic peaks were obtained, while peaks corresponding to the liquidus line were weak. In Fig.1(a), the peritectic and eutectic reaction temperatures observed on heating and cooling curves were plotted against different  $\text{TiO}_2$  concentrations. The eutectic and the peritectic temperatures were determined to be  $823 \pm 3^\circ\text{C}$  and  $855 \pm 2^\circ\text{C}$ , respectively. Surprisingly, the temperatures corresponding to the eutectic reaction were higher and the temperatures corresponding to the peritectic reaction were lower than those reported by Bruton<sup>5)</sup> as shown in Fig.1(b).

Hereafter, we focus on a  $\text{TiO}_2$ -poorer region than the stoichiometric BTO, because the single crystals are grown only from hypo-peritectic solutions using the TSSG pulling. According to Bruton's phase diagram shown in Fig.1(b), starting solutions with a  $\text{TiO}_2$  concentration of lower than the peritectic composition ( $\sim 12$  mol%) provide the BTO single phase. Since clear peaks corresponding to the liquidus temperature close to the peritectic composition could not be obtained on DTA curves, TSSG pulling was carried out with 10.25 to 11.25 mol%  $\text{TiO}_2$  solutions in order to verify the peritectic composition. Polycrystalline boules consisting of  $\text{Bi}_2\text{O}_3$ , BTO and  $\text{Bi}_4\text{Ti}_3\text{O}_{12}$  were obtained from 11.00 and 11.25 mol%  $\text{TiO}_2$  solutions, while single phase BTO crystals were obtained from 10.25 and 10.50 mol%  $\text{TiO}_2$  solutions. As shown in Fig.2(a), the boule grown from a 10.75 mol%  $\text{TiO}_2$  solution indicated by the arrow in Fig.1(a) looked polycrystalline (dominantly  $\text{Bi}_4\text{Ti}_3\text{O}_{12}$ ), but the inside more than 95% of the lower half part shown in (b) was recognized to be a monocrystalline BTO phase with a lattice constant of  $10.1743_9 \text{ \AA}$ . This means that the first crystallized part beneath the seed crystal was of the lamellae-type  $\text{Bi}_4\text{Ti}_3\text{O}_{12}$  phase and the BTO single phase crystallization after the while resulted from a gradual change in solution composition passing the peritectic composition along the liquidus curve. Therefore, we emphasize that the substantial peritectic composition must lie close to a 10.75 mol%  $\text{TiO}_2$  concentration or less to some degree.

### 3.2 Lattice constant of the $\text{Bi}_{12}\text{TiO}_{20}$ phase in ceramics

Figure 3 shows the lattice constants of the BTO phase in the calcined ceramics as a function of  $\text{TiO}_2$  concentration in nominal mol%, redrawn from our early work<sup>11)</sup>. The measurements were carried out more than 3 times for each sample. X-ray diffraction patterns of samples with a  $\text{TiO}_2$  of less than the stoichiometric 14.28<sub>6</sub> mol%  $\text{TiO}_2$  (hypo-peritectic region) showed the existence of  $\alpha$ - $\text{Bi}_2\text{O}_3$  phase, while those of the samples exceeding 14.28<sub>6</sub> mol%  $\text{TiO}_2$  (hyper-peritectic region) included relatively small signals of  $\text{Bi}_4\text{Ti}_3\text{O}_{12}$ . As  $\text{TiO}_2$  concentration increased from 13.3 mol%,

the lattice constant decreased monotonously and seemed to reach a minimum at around 13.80~13.85 mol%  $\text{TiO}_2$ . From this minimum, the lattice constant increased rapidly to about a maximum value at around 14.2 mol%  $\text{TiO}_2$  and again decreased for 14.7 mol%  $\text{TiO}_2$  through the stoichiometric composition (14.28<sub>6</sub> mol%  $\text{TiO}_2$ ). This strongly indicates the existence of a non-stoichiometric solid solution range. Besides, we noticed that the lattice constant of the stoichiometric compound was necessarily smaller than that of the BTO phase in the 14.2 mol%  $\text{TiO}_2$  compound. Such a non-linear relationship between the solution composition and the lattice constant of crystals was also discussed in  $\text{Bi}_{12}\text{SiO}_{20}$  (BSO)<sup>12</sup>, where the composition of a crystal grown from  $x \sim 11.6$  melt composition in the formula of  $\text{Bi}_x\text{SiO}_{1.5x+2}$  showed the minimum<sup>13</sup>.

It can be readily supposed that there exists a solid solution in the hypo-peritectic region. Bruton's phase diagram (shown in Fig.1(b)) indicates that a BTO crystallizes as the primary phase from a  $\text{Bi}_2\text{O}_3$ -rich solution in the hypo-peritectic region and the crystal composition is independent of the solution compositions. However, a rapid increase of lattice constants in the hypo-peritectic region suggests that the stoichiometry of the primarily crystallized BTO must be influenced by a starting solution composition. Figure 4(a) shows the calculated lattice constants of BTO single crystals grown in succession from each starting solution of 4.0, 5.0, 6.5, 8.0, 9.0 and 10.25 mol%  $\text{TiO}_2$ , where one point data of the crystals grown from 10.10 and 10.75 mol%  $\text{TiO}_2$  (see Section 3.1) solutions are added. The lattice constant decreased monotonously with an increased  $\text{TiO}_2$  concentration, but those of crystals grown from a 9.0 mol%  $\text{TiO}_2$  solution show the minimum. Noticeably, the lattice constants of crystals grown from 8.0 and 10.25 mol%  $\text{TiO}_2$  solutions are larger than that grown from a 9.0 mol%  $\text{TiO}_2$  solution and are almost the same. This means that the crystal compositions grown from 8 and 10.25 mol%  $\text{TiO}_2$  solutions must be very close to each other, and this strongly suggests that a solidus curve must be retrograde, regardless of point defects such as  $\text{Bi}_{\text{Ti}}^{3+}$ -antisites<sup>14</sup>, vacancies and/or oxygen deficiency.

### 3.3 Retrograde phase relation of the solid solution

The standard deviation of calculated lattice constants of the single crystals grown from each solution was taken into account in drawing the solidus line of a solid solution. This is because the composition of the primarily crystallized phase corresponds predominantly to the solidus line in phase equilibrium. As shown in Fig.4(b), the deviation of lattice constants of the crystals grown from the 9.0 mol%  $\text{TiO}_2$  solution showed a minimum value of  $2.67 \times 10^{-5} \text{ \AA}$ . This means that the corresponding solidus line changes its slope ( $dT/dC_s$ , where T is the temperature and  $C_s$  is the  $\text{TiO}_2$  concentration) from a positive to a negative one. On the other hand, the lattice constant deviation of other crystals became larger to some degree, which implies a gentle slope of the solidus line, especially that from a 10.25 mol%  $\text{TiO}_2$  is relatively large. Therefore, it can be said that the crystal composition grown from a 9.0 mol%  $\text{TiO}_2$  solution must correspond to the turning point of a retrograde solidus curve, even when the starting solution composition changes to some degree by the successive adding of a stoichiometric compound equal in weight to that of the previously grown crystal. This proves the minimum deviation of lattice constants of the crystals grown from the 9.0 mol%  $\text{TiO}_2$  solution.

Together with experimental results and the expected considerations described above, it is possible to draw the relevant part of the phase diagram in the hypo-peritectic region close to the stoichiometric composition of a BTO (14.28<sub>6</sub> mol%  $\text{TiO}_2$ ). Figure 5 shows a renewed, substantial phase diagram with a plausible retrograde solid solution close to the stoichiometric BTO. We can consider that the turning point of the retrograde solidus curve lies around 13.80~13.85 mol%  $\text{TiO}_2$ , because the minimum value in Fig.3 lies around 13.80~13.85 mol%  $\text{TiO}_2$ . This retrograde characteristic can explain qualitatively the lattice constant variation shown in Fig.3, and is very similar to that in the solid solution regime of congruently melting  $\text{Bi}_{12}\text{SiO}_{20}$ <sup>12)</sup>, and will be clarified in Chapter 4.

As is expected from Figs.4 and 5, we can clearly understand that the standard deviation of the lattice constants of crystals grown from a 9.0 mol%  $\text{TiO}_2$  solution had the lowest ( $2.67 \times 10^{-5} \text{ \AA}$ ), while those grown from lower  $\text{TiO}_2$  mol% solutions were larger than  $5 \times 10^{-5} \text{ \AA}$ . This means that a very



high reproducibility of the crystal composition from the 9 mol%  $\text{TiO}_2$  solution is to be expected. We achieved reproducible growth of high quality BTO single crystals (relatively the same lattice constant) by adding stoichiometric ceramics equal in weight to that of the previously grown crystal<sup>15</sup>).

#### 4. Growth of long single crystals

As was discussed in Section 3.3, an about 9.0 mol%  $\text{TiO}_2$  solution was determined to be the best starting solution for the reproducible growth of relatively small single crystals, resulting in almost the same lattice constant. In the case of TSSG pulling, the starting solution composition changes gradually along the liquidus line as a crystal grows up. Then, the variation of the lattice constant along the crystal length was investigated by growing long single crystals.

First, an about 55 mm long and 147.7 gr weighed single crystal was grown from a fresh 9.0 mol%  $\text{TiO}_2$  solution, as shown in Fig.6. Lattice constants at the top and bottom were measured to be  $10.1738_7$  and  $10.1747_0 \text{ \AA}$ , respectively. The lattice constant of the primarily crystallized top corresponds well to that of crystals grown from the 9.0 mol%  $\text{TiO}_2$  solution and that of the bottom is close to that of a crystal grown from a 6.7 mol%  $\text{TiO}_2$  solution, as is deduced from Fig.4(a). This tendency accords fairly well with the retrograde solidus curve; the  $\text{TiO}_2$  concentration in the solution becomes gradually poorer along the liquidus line as the crystal grows up, and the corresponding  $\text{TiO}_2$  concentration in the crystal becomes richer along the solidus line, resulting in an increase in the lattice constant, as shown in Fig. 4(a).

Second, an about 53 mm long and 123.9 gr weighed single crystal was grown from a 10.0 mol% solution. Figure 7 shows the as-grown crystal, where the lattice constants of ① the first crystallized part, ② the upper part of the boule, ③ the lower part of the boule, and ④ the bottom part were evaluated to be  $10.1741_7$ ,  $10.1739_0$ ,  $10.1745_5$ , and  $10.1752_5 \text{ \AA}$ , respectively. This change in lattice constants along the growth axis follows the retrograde solidus line shown in Fig.5 reasonably well. The lattice constants of the parts

①, ②, ③, and ④ correspond to crystals grown from 10.00~10.1 mol%, ~9.8 or 8.6 mol%, ~7.1 mol%, and ~6.1 mol%  $\text{TiO}_2$  solutions, respectively, as are deduced from Fig.4(a).

The single crystal grown from the 9.0 mol%  $\text{TiO}_2$  solution had a solidified fraction of 65.8%, since a total amount of solution charged into a crucible was 373.72 gr from which a BTO crystallizes 224.3 gr in weight. On the other hand, the crystal grown from the 10.0 mol%  $\text{TiO}_2$  solution had a solidified fraction of 49.7%, since the total amount of solution was 370.4 gr from which a BTO crystallizes 249.2 gr in weight. In referring to Fig. 4, single crystals grown from solutions with  $\text{TiO}_2$  concentrations of between ~7.5 and ~10.0 mol% have a lattice constant deviation of less than  $\sim 1.0 \times 10^{-4} \text{ \AA}$ . Consequently, it can be said that a starting solution with a 10.0~10.10 mol%  $\text{TiO}_2$  is very practical for growing relatively homogeneous single crystals whose lattice constants are within  $\pm 1 \times 10^{-4} \text{ \AA}$  over the whole crystal boule, as indicated by the shadow bar in Fig.5, when a solidified fraction is at least less than 45% for this purpose.

## 5. Refractive index measurement

Figure 8 shows wavelength dispersion of the refractive index of the thus grown crystals. This is the first result on the refractive index of a BTO single crystal. The dispersion fits well with the single-term Sellmeier's relation

$$n^2 - 1 = S_0 \lambda_0^2 / [1 - (\lambda_0 / \lambda)^2], \quad (1)$$

where  $S_0$  is the average oscillator strength, and  $\lambda_0$  is the average oscillator position. Using a straight-forward approximation,  $S_0$  and  $\lambda_0$  were determined to be 94.1265 and 0.227135, respectively. We can then express Eq.(1) as

$$n^2 - 1 = 4.8560_2 / [1 - (0.2271_3 / \lambda)^2]. \quad (2)$$

As far as we know, this is the first report of the wavelength dependence of the refractive index of a BTO single crystal. The value is larger than that of a BSO<sup>16)</sup>, and then the product  $n^3 r_{41}$  ( $\lambda = 6.328$

nm) of a BTO was estimated to be more than 1.3 times that of a BSO, although the wavelength dependence of the electro-optic constant is unknown. Knowing the correct refractive index is very important because of its use in preparing anti-reflection coating and high-reflective coating mirrors on either end of an EOS chip.

The voltage sensitivity was measured with a 1 V, 100 MHz sinusoidal signal on a standard micro-strip line, and a handy-type EOS system with a probe head made of a BTO crystal has 1.5 times higher voltage sensitivity than one made with a BSO crystal<sup>3, 17)</sup>. Figure 9 shows the measured result illustrating an improvement in voltage sensitivity of more than 1.5 times higher than that of a BSO head with precise manipulation. Since the shot-noise-limited expression for a minimum detectable voltage  $V_{\min}$  is given by Eq.(1) where  $V_{\pi}$  is inversely proportional to  $n^3r$ , the increase in sensitivity can be analyzed semi-quantitatively as follows, even though there is a lack of accurate values;  $r_{41}$  of a BTO is 1.15~1.4 times larger<sup>4)</sup>,  $n$  is about 1.04 times and  $\epsilon$  is about 0.8 times larger than those of a BSO, that yields at least a  $\sim 1.5$  times larger  $n^3r_{41}/\epsilon$  than that of a BSO. So, a 1.5 times improvement in voltage sensitivity shown in Fig.9 is reasonable. In this advanced and practical system, the use of a BTO crystal as a probe head was one of the key issues inevitable for improvement of voltage sensitivity<sup>18)</sup>. So the reproducible growth of the single crystal described in this paper is very effective for practical uses as an EOS probe head, and is also very useful in photorefractive applications.

## 7. Summary

For practical application of a sillenite  $\text{Bi}_{12}\text{TiO}_{20}$  (BTO) crystal to a handy-type, high-impedance electro-optic sampling probe system, we renewed the phase diagram of the hypo-eutectic  $\text{Bi}_2\text{O}_3$ - $\text{TiO}_2$  region and characterized BTO single crystals by measuring the lattice constants of crystals grown from hypo-peritectic solutions by using the TSSG method. This study strongly proved the existence

of a solid solution region with a retrograde solidus curve whose turning point lies around 13.80~13.85 mol%  $\text{TiO}_2$ , corresponding to an about 9.0 mol%  $\text{TiO}_2$  solution. From a 9.0 mol%  $\text{TiO}_2$  solution, BTO single crystals with a minimum lattice constant deviation of less than  $3 \times 10^{-5} \text{ \AA}$  could be reproducibly grown. A starting solution with a 10.0~10.1 mol%  $\text{TiO}_2$  concentration and the solidified fraction of the crystal of less than about 45% will result in a relatively homogeneous single crystal whose lattice constant deviation is less than  $1 \times 10^{-4} \text{ \AA}$ .

The wavelength dispersion of the refractive index was measured for the first time, and the product  $n^3r$  of a BTO was estimated to be about 1.3 times larger than that of BSO. The improvement in voltage sensitivity in the handy-type EOS system by replacing a BSO with a BTO for a probe head was basically associated with this increase in  $n^3r/\epsilon$ .

This paper presented the first experimental results showing the existence of a retrograde solid solution of incongruently melting BTO, which is representative of the peritectic decomposition binary system. Because the stoichiometry of these crystals should be poorer in  $\text{TiO}_2$  concentration than in stoichiometric BTO ones, we are now investigating the crystal chemistry of off-stoichiometric BTO single crystals grown from different starting solutions.

#### Acknowledgments

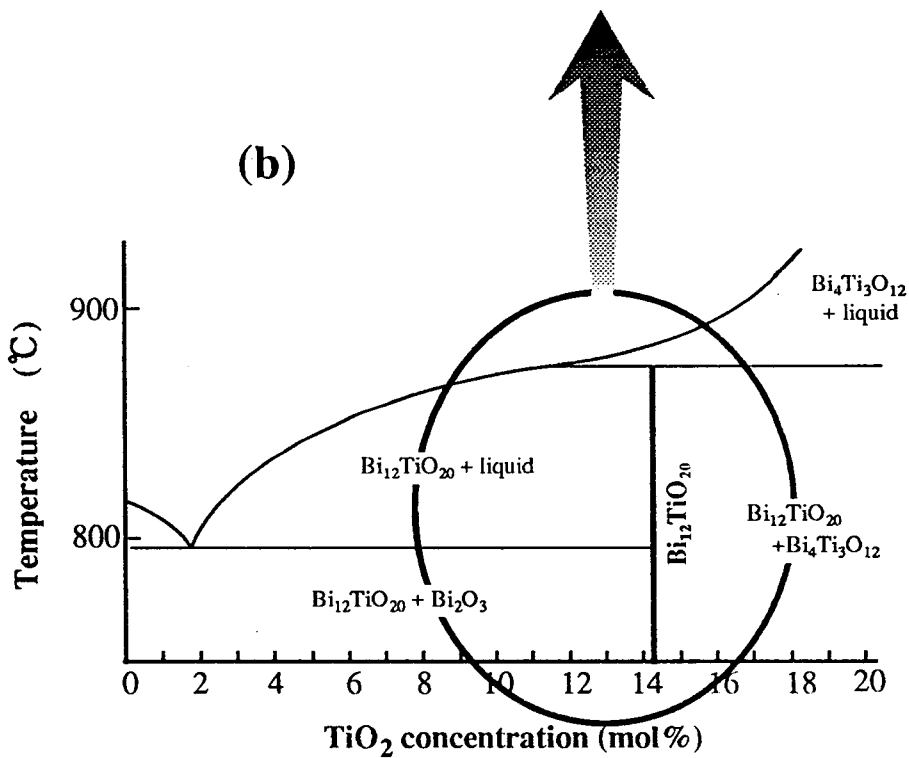
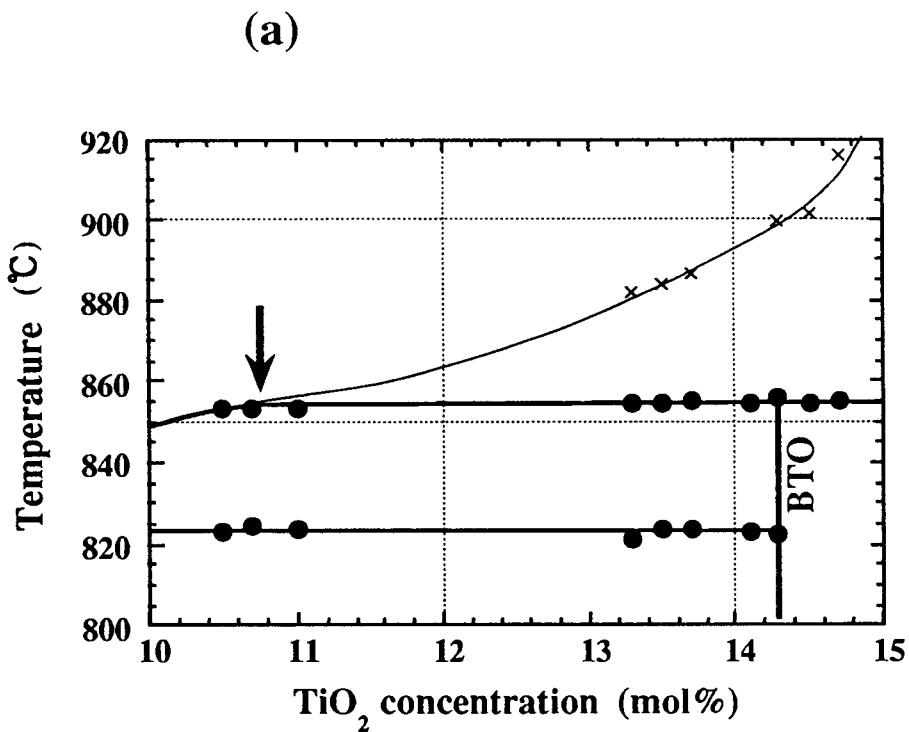
Most of this work was done, when the author had been in NTT System Electronics Labs. till March, 1998. The author wishes to express his thanks to N.Suzuki (USHIO Research Institute of Technology Inc.) and T. Tabata (NTT Advanced Technology Corp.) for their crystal growth experiments and lattice constant measurements, and to Drs.M.Shinagawa and T.Nagatsuma for their EOS measurements.

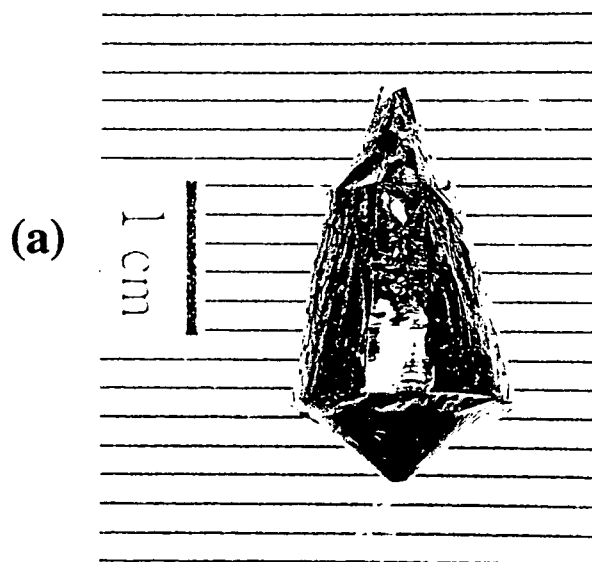
## References

- 1) K.J.Weingarten, M.J.Rodwell and D.M.Bloom ; IEEE J.Quant.Electron., QE-24 (1988) 198
- 2) M.Shinagawa and T.Nagatsuma ; IEEE Trans.Instr.& Meas., 43 (1994) 843
- 3) M.Shinagawa and T.Nagatsuma ; IEEE Trans.Instr.& Meas., 45 (1996) 575
- 4) J.P.Wilde, L.Hesselink, S.W.McCarhon, M.B.Klein, D.Rytz and B.A.Wechsler ; J.Appl.Phys., 67 (1990) 2245
- 5) T.M.Burton; J.Sol.Sta.Chem., 9 (1974) 173
- 6) T.M.Bruton, J.C.Brice, O.F.Hill and P.A.C.Whiffin; J.Cryst.Growth, 23 (1974) 21
- 7) D.Rytz, B.A.Wechsler, C.C.Nelson and K.W.Kirby; J.Cryst.Growth, 99 (1990) 864
- 8) Y.Okano, H.Wada and S.Miyazawa; Jpn.J.Appl.Phys., 30 (1991) L1307
- 9) S.Miyazawa; Opt. Mat., 4 (1995) 192
- 10) S.Miyazawa; J.Cryst.Growth, 167 (1996) 638
- 11) S.Miyazawa and T.Tabata; J.Cryst.Growth (in press, 1998)
- 12) J.C.Brice, M.J.Hight, O.F.Hill and P.A.C.Whiffin; Philips Tech.Rev., 37 (1977) 250
- 13) O.F.Hill and J.C.Brice, J.Mater.Sci., 9 (1974) 1252
- 14) R.Oberschmid, Phys.Sta.Sol.(a), 89 (1985) 263
- 15) S.Miyazawa and T.Tabata, NTT REVIEW, 10 (1998) 62
- 16) R.E.Aldrich, S.L.Hou and M.L.Harvill ; J.Appl.Phys., 42 (1971) 493
- 17) M.Shinagawa and T.Nagatsuma; Proc.of 1997 IEEE Instr. & Meas. Technol.Conf. (19~21 May, 1997, Ottawa, Canada), T34-2
- 18) M.Shinagawa, T.Nagatsuma and S.Miyazawa ; IEEE Trans.Instr. & Meas., 47 (1998) 235

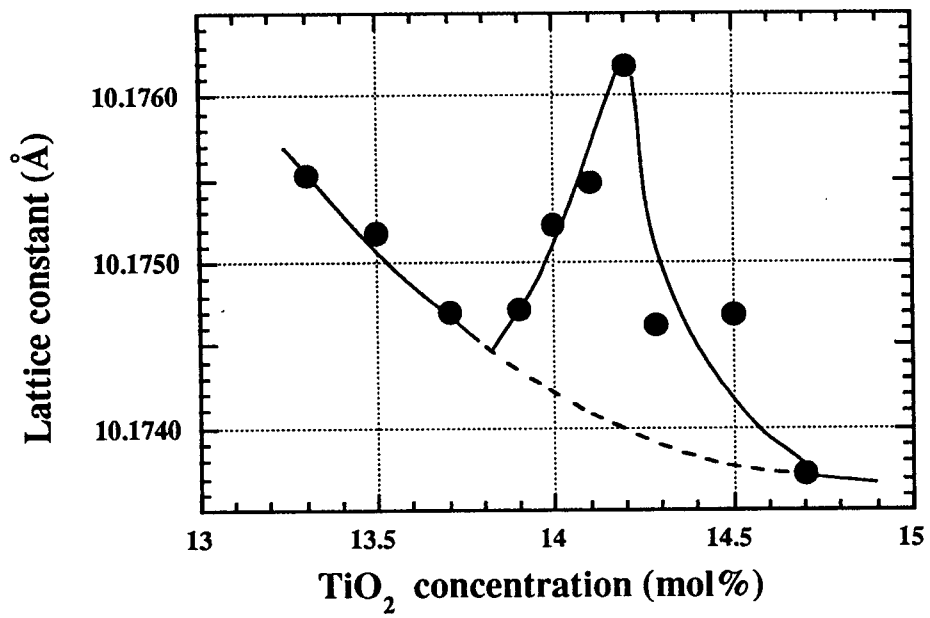
## Figure captions

- Figure 1 (a) Substantial phase diagram based on DTA and crystal growth experiments. A crystal boule grown from the solution (10.75 mol%), indicated by the arrow, contained  $\text{Bi}_4\text{Ti}_3\text{O}_{12}$  phase and  $\text{Bi}_{12}\text{TiO}_{20}$  single crystal (see text and Fig.2), and (b) the phase diagram reported by Bruton<sup>5</sup>).
- Figure 2 (a) A picture of a boule grown from the 10.75 mol%  $\text{TiO}_2$  solution, and (b) the inner part of the lower half part of the boule showing single crystalline BTO blocks.
- Figure 3 Lattice constant variation of the BTO phase in calcined ceramics as a function of  $\text{TiO}_2$  nominal concentration.
- Figure 4 (a) Lattice constant of single crystals against  $\text{TiO}_2$  concentration in solution. Each crystal was grown from a solution by adding a stoichiometric BTO ceramic equal in weight to that of the previously grown crystal, and (b) standard deviation of lattice constants of single crystals against a  $\text{TiO}_2$  mol% in solution. The shaded bar indicates usable solutions for obtaining homogeneous crystals (see text).
- Figure 5 Substantial  $\text{Bi}_2\text{O}_3$ – $\text{TiO}_2$  binary phase relation in the hypo-peritectic region of a BTO. From the solutions of 10.10~8.0 mol%  $\text{TiO}_2$ , the crystal composition lies in the shaded area,  $13.85 \pm 0.05$  mol%  $\text{TiO}_2$ .
- Figure 6 Long single crystal (right) and a typical crystal (left) grown from a 9.0 mol%  $\text{TiO}_2$  solution.
- Figure 7 Long single crystal grown from a 10.0 mol%  $\text{TiO}_2$  solution from which lattice constants at ①, ②, ③, and ④ were measured (see text).
- Figure 8 Wavelength dispersion of the refractive index of reproducibly grown BTO crystals.,
- Figure 9 The improvement of voltage sensitivity using a BTO crystal head, as compared with the case using a BSO<sup>18</sup>).

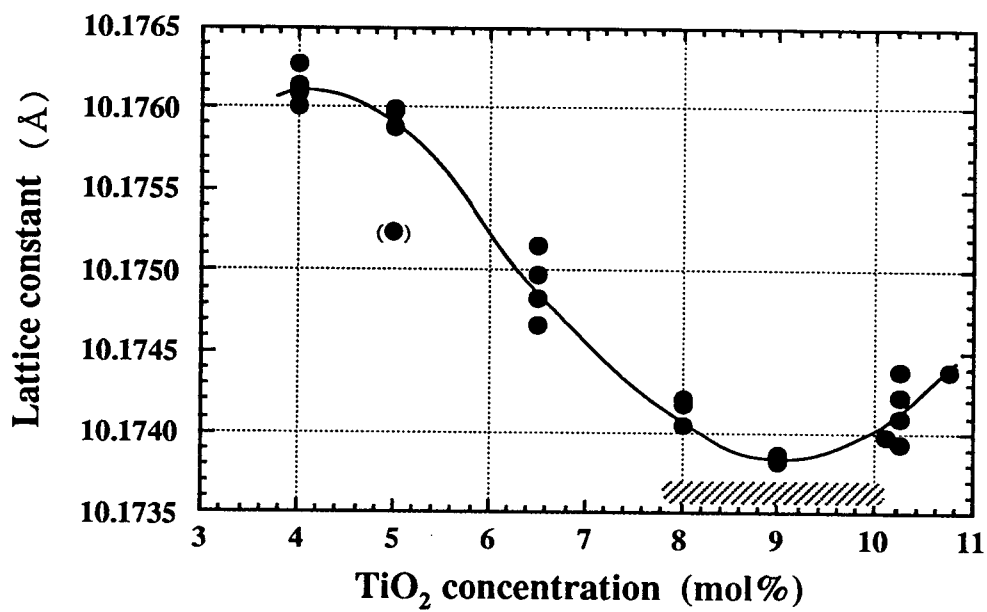








(a)



(b)

